SSRG International Journal of Thermal Engineering
ISSN: 2395-0250/ https://doi.org/10.14445/23950250/IJTE-V11I2P102

Volume 11 Issue 2, 11-15, May-Aug 2025

Original Article

Heat Transfer, Fluid Mechanics and Energy Analysis of an Industrial Roller Ironing Machine

Sercan Acarer[1], Kader Sever[2], Can Çivi[3]

[1]*İzmir Katip Çelebi University, İzmir, Türkiye.*
[2]*Tolkar Inc., İzmir, Türkiye.*
[3]*Manisa Celal Bayar University, Manisa, Türkiye.*

[1]*Corresponding Author : sercan.acarer@ikcu.edu.tr*

Received: 28 April 2025 Revised: 02 June 2025 Accepted: 19 June 2025 Published: 07 July 2025

Abstract *- In this study, energy, heat transfer, and fluid flow analyses were conducted for an industrial roller ironer, a system that has received limited attention in the scientific literature. These machines simultaneously dry and press flat textiles by conveying them between a rotating roller and a stationary heated chest. A high and uniform surface temperature is maintained via thermal oil circulation within the chest, enabling rapid moisture evaporation and fabric smoothing. This system is widely employed in industrial laundries for high-throughput ironing. Two operating conditions are considered, one with pre-dried fabric (faster ironing) and one without pre-drying (slower ironing), both requiring the same heat load. A single Conjugate Heat Transfer (CHT) CFD simulation was performed under this heat load to represent both scenarios. The simulations yielded the surface heat load and temperature distribution, revealing localized regions of low heat flux. These zones were attributed to complex three-dimensional flow separation occurring at the U-bends of the internal oil channels, which impair local heat transfer. Design modifications were proposed to mitigate these deficiencies. Overall, the analysis indicates uniform thermal performance across the ironing surface, with targeted areas for further improvement.*

Keywords *- Heat transfer, CHT, CFD, Industrial Ironer, Thermal Oil Heated Flatwork Ironer.*

1. Introduction

The textile industry is a fragmented and heterogeneous complex manufacturing industry dominated by small and medium-sized enterprises. The industry consists of production equipment that often uses old traditional technologies, thus leading to huge energy consumption [1]. Industrial laundries, which are one of the important elements of this sector, are establishments that industrially treat linen by cleaning it from a variety of sources, such as hospital sheets, hotel linens, restaurant towels and tablecloths, work clothes and working uniforms, shop towels, and textiles from beauty salons. The ironing process is one of the most important steps in industrial laundry [2]. In addition, the ironing process is also an important part of textile production. It stands out as the final step in the process of textile production. The process consumes a large amount of energy, and ironing has a structure that requires the correct selection of process parameters to be carried out correctly [3]. Electricity or natural gas energy is used to obtain the necessary energy in the ironing process [4]. Electrical energy is the primary energy source used in ironing as well as in the entire textile processing industry [5]. Today, the issue of reducing energy consumption and, therefore, carbon footprint is gaining importance day by day due to energy scarcity and environmental awareness, which has emerged in recent years. Analysis and studies within this framework have become very valuable for all basic process steps of the textile industry [6], [7], [8]. From the perspective of the ironing process, almost no studies have been done in this context. The systems considered are simple household irons or semi-industrial systems based on a fixed and moving plate, rather than industrial ironing systems [9], [10], [11].

Despite the widespread use of industrial roller ironers in textile production and laundry operations, there is a notable lack of detailed thermal and fluid dynamic analysis for these systems in the literature. Achieving uniform heat transfer across the ironing surface is essential for consistent fabric quality and energy efficiency, yet the impact of internal flow structures and design parameters on thermal performance remains poorly understood. This study aims to fill this gap by performing a Conjugate Heat Transfer (CHT) CFD analysis of an industrial ironing unit under representative operating conditions. The objective is to reveal the internal flow behavior and surface heat transfer characteristics, identify thermally underperforming regions, and propose design strategies to enhance system efficiency and ironing uniformity.

2. Materials and Methods

2.1. System Description

The industrial roller ironer investigated in this study is designed to simultaneously dry and press flat textiles by conveying them between a rotating roller and a stationary, heated chest (Figure 1). Uniform and elevated surface temperatures are achieved by circulating thermal oil within the chest, enabling efficient moisture evaporation and effective fabric smoothing. This type of system is widely employed in industrial laundries for high-throughput ironing operations. The ironing unit features a semi-cylindrical surface, internally heated by thermal oil that flows through embedded U-shaped channels. The oil enters through a centrally located supply port and is discharged symmetrically from outlets positioned at both ends.

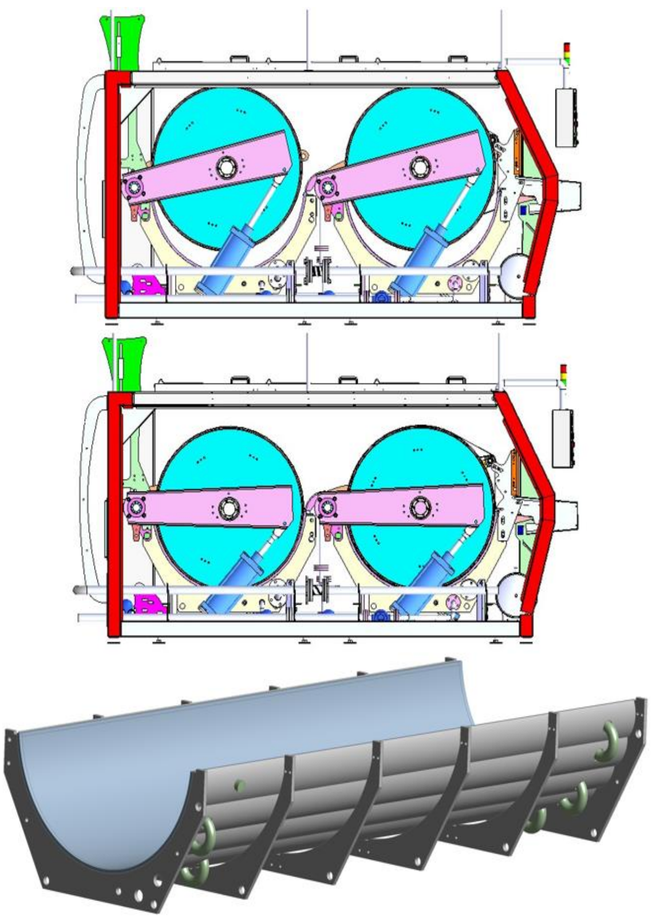

Fig. 1 The multi-stage ironing system with open (top) and closed (central) positions and the heated chest of the ironer (bottom)

These design elements are depicted in the CFD model shown in Figure 2. To represent realistic thermal behavior, the bottom side of the unit is assumed to be well insulated to minimize heat loss. The CFD model accounts for the complex three-dimensional flow structures and associated heat transfer within the internal passages, which are critical to achieving thermal uniformity across the ironing surface.

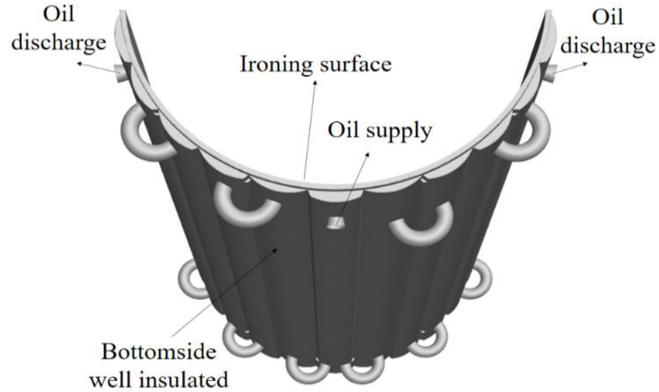

Fig. 2 The CFD model

The computational domain was discretized using an unstructured polyhedral mesh with inflation layers near the solid–fluid interfaces to accurately capture thermal boundary layer effects. The wall function approach is employed so that y+ is around 40 on the fluid walls. The mesh includes the internal U-shaped thermal oil channels, the solid chest walls, and the ironing surface. A denser mesh was applied in critical regions such as the curved U-bends and the fabric contact surface to resolve complex flow separation and steep thermal gradients. The mesh quality was assessed through the skewness metric, which is around 0.95 for the worst volume. The total mesh size is 8x10^6 volumes.

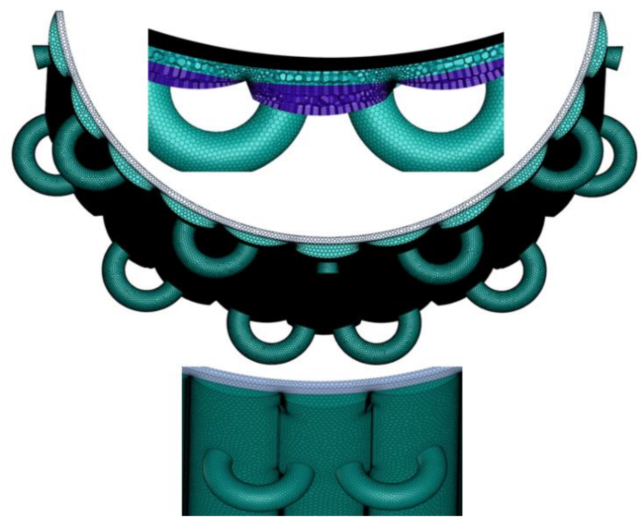

Fig. 3 The computational mesh

2.2. Energy Analysis

Two operating conditions are considered for the ironing process. In the first scenario, pre-drying is applied, leading to an initial moisture content of 25%, a final moisture content of 13%, and a fabric feed speed of 55 m/min. In the second scenario, no pre-drying is employed, resulting in a higher initial moisture content of 45%, while maintaining the same final moisture content of 13% and a reduced feed speed of 25 m/min. The operating parameters for both cases are summarized in Table 1.

Table 1. The two operating conditions for the ironer

	Initial moisture	Final moisture	Feed Speed
With pre-drying	25%	13%	55m/min
Without pre-drying	45%	13%	25m/min

Assumptions and other knowns are given below:

- Dry fabric mass per unit area is 0.1 kg/m²
- Fabric is heating from 25°C to 100°C, with specific heat of 1.3 kJ/kg·K
- Latent heat of vaporization (h_{fg}) is taken as 2256.4 kJ/kg, corresponding to the value at 100°C under approximately 1 atm pressure.
- Material properties for the thermal oil and steel are taken as constant at the operating temperature of 200 ˚C and given in Table 2.
- The thermal oil flow rate is 45 m³/h at 200 ˚C supply temperature.

Table 2. Material properties

	Thermal Oil	Steel
Density (kg/m³)	868	7850 (not needed)
Specific Heat (J/kg.K)	1860	430 (not needed)
Thermal Conductivity (W/m.K)	0.133	23
Dynamic Viscosity (Pa.s)	6.6×10^{-4}	-

In order to calculate heat loads under two scenarios, the following equations are used:

The water to be evaporated per unit area is calculated by Eq.(1):

$$m''_{evaporated} = m''_{dry} * (X_{in} - X_{out}) \tag{1}$$

The required thermal energy for evaporation is calculated by Eq.(2):

$$q_{evaporation} = m''_{evaporated} * h_{fg} \tag{2}$$

Energy for heating fabric is calculated by Eq.(3):

$$q_{fabric} = m''_{dry} * c_p * \Delta T \tag{3}$$

Total energy per unit area is calculated by Eq.(4):

$$q_{total} = q_{evaporation} + q_{fabric} \tag{4}$$

Considering the time for 1 m² of fabric to pass $\Delta t = 1/V$, the surface heat load is finally obtained by Eq.(5):

$$\dot{q}_{total} = q_{total}/\Delta t \tag{5}$$

The calculations performed using Equations (1)–(5) yield the results in Table 3. Although the total energy requirements differ between the two cases, the variation in feed speed results in comparable energy rates (power requirements), both approximately 34 kW/m².

Table 3. Heat load calculation results

	With pre-drying	Without pre-drying
Energy for evaporation (kJ/m²)	27.08	72.20
Energy for heating fabric (kJ/m²)	9.75	9.75
Total energy (kJ/m²)	36.83	81.95
Heat load (kW/m²)	33.76	34.18

3. Results and Discussion

The CFD results depicted in Figure 4 indicate a non-uniform heat flux distribution across the ironing surface with an average value of 34 kW/m2 for a surface temperature of 157 ˚C. Since these are in line with the actual 160 ˚C observed during operation, CFD analyses are assessed as valid. While large portions of the surface exhibit elevated heat flux values in the 45–55 kW/m² range, several localized regions show significant reductions, with values dropping to as low as 10–25 kW/m². These low-flux zones are observed predominantly along the sides, notably in the spaces between adjacent internal heating channels. The reduced heat flux in these inter-channel regions is attributed to less effective convective heat transfer due to diminished thermal oil flow coverage. Additionally, recirculation and flow separation effects, particularly in the U-bend sections of the oil circuit, further impair heat transfer in certain areas.

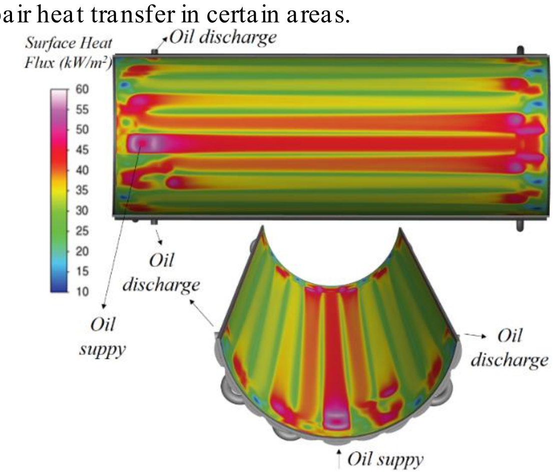

Fig. 4 Heat flux distribution on the ironing surface

Figure 5 illustrates the internal flow behavior of thermal oil through the U-shaped heating channels of the ironing unit, providing insight into the root causes of these non-uniformities observed in Figure 4. Pathlines are colored according to local oil temperature, revealing the temperature distribution and mixing characteristics throughout the flow domain. The oil enters from the centrally located supply port at elevated temperature (200 °C), then splits into two branches, flowing almost symmetrically toward both ends of the system and discharging at a temperature of 190 °C.

The central channel maintains high temperatures with strong convection (see Figure 4). However, in the peripheral regions, particularly within the U-bends at both ends, recirculation zones and flow separation are observed. These features result in extended residence times and increased thermal losses.

Such regions contribute to the reduced heat flux observed on the corresponding areas of the ironing surface (Figure 4).

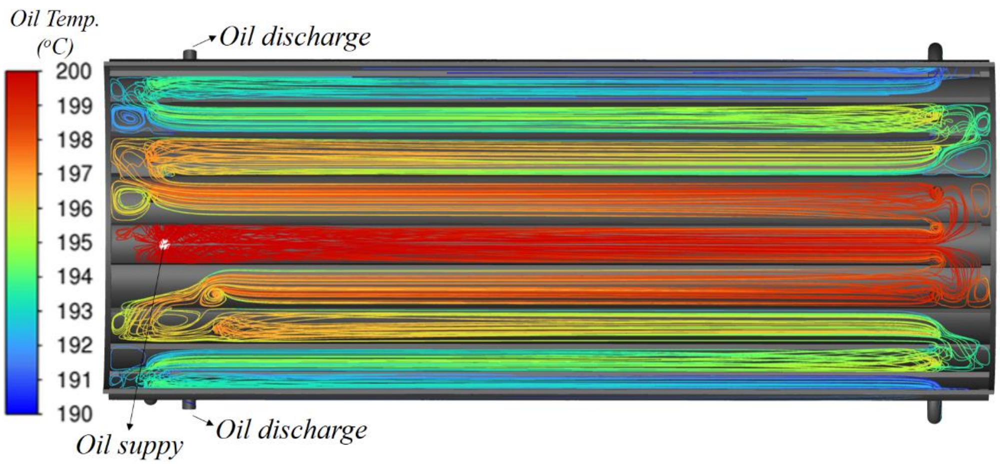

Fig. 5 Flow pathlines of the thermal oil within the ironing chest, colored by oil temperature

The distribution of wall shear stress across the channel walls, illustrated in Figure 6, provides insights into the local fluid friction experienced by the surface. As seen in the figure, the highest shear stresses occur predominantly in the central straight channel sections, where the flow is well-developed and aligned with the main axis of the channel. These regions experience strong axial flow, resulting in sustained shear and heat transfer at the wall.

In contrast, low-shear zones are evident near the U-bends, especially around inlet and outlet junctions, and at the curved return corners, where flow recirculation and separation are likely present. These regions are characterized by irregular flow patterns and reduced wall-parallel velocity components, leading to diminished wall shear stress.

The non-uniform distribution of shear stress suggests that while most of the heat transfer is supported by the strong shear-driven convection in the straight sections, the U-bend regions may become thermally underperforming due to lower fluid friction and poorer local heat transfer.

Figure 7 illustrates the corresponding pressure field of the circulating thermal oil within the internal channel network. The oil is supplied at the central inlet, and the pressure gradually decreases along the flow path toward the discharge ports on both ends. This pressure gradient is responsible for driving the oil through the U-shaped channels embedded in the chest wall. A relatively symmetric pressure drop is observed across the upper and lower branches of the system, although minor asymmetries arise due to geometric features and secondary flows.

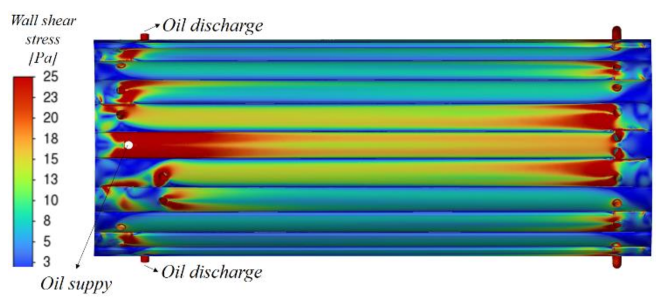

Fig. 6 Wall shear stress distribution along the inner surfaces of the U-shaped heating channels

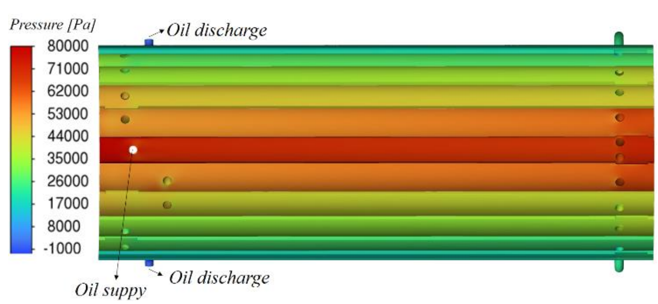

Fig. 7 Pressure distribution on the inner channel walls of the ironing chest

4. Conclusion

In this study, a numerical investigation was carried out on an industrial thermal oil-heated roller ironer widely used in textile manufacturing and laundry applications. By integrating energy balance calculations with Conjugate Heat Transfer (CHT) CFD simulations, the thermal performance and internal flow characteristics of the system were evaluated under two representative operating conditions. Although the total energy requirements varied due to differences in fabric moisture content and feed speed, the resulting surface heat loads were found to be comparable, both approximately 34 kW/m².

The CFD results indicated that while the ironing surface generally achieves high and uniform heat flux, localized regions with reduced thermal performance persist, particularly along the side boundaries and between adjacent internal channels. Flow pathline visualizations and wall shear stress distributions revealed that these thermal inefficiencies are primarily driven by complex three-dimensional effects, including recirculation and flow separation near the U-bends and junctions of the internal oil channels.

Based on the insights gained, several design improvements are proposed to enhance thermal uniformity and overall system efficiency. These include the integration of flow-guiding vanes to mitigate recirculation zones, cross-sectional adjustments or equalization features to improve flow distribution in inter-channel regions, and geometric modifications to increase flow penetration into peripheral channels. Furthermore, replacing the single central oil supply with a multi-port distribution system could help minimize axial gradients in temperature and pressure, thereby improving thermal uniformity. Collectively, these recommendations aim to improve surface heat flux homogeneity, ironing performance, and energy efficiency, without compromising the fundamental operational principles of the existing design.

Acknowledgments

The authors would like to thank TOLKAR-Smartex for their support in preparing this work.

References

[1] Ali Hasanbeigi, and Lynn Price, "A Review of Energy Use and Energy Efficiency Technologies for the Textile Industry," *Renewable and Sustainable Energy Reviews*, vol. 16, no. 6, pp. 3648-3665, 2012. [CrossRef] [Google Scholar] [Publisher Link]

[2] Grégorio Crini et al., "Characterization and Treatment of Industrial Laundry Wastewaters: A Review," *Environmental Chemistry Letters*, vol. 22, pp. 2257-2292, 2024. [CrossRef] [Google Scholar] [Publisher Link]

[3] D. Rogale and S. FirštRogale, "Energy and Environmental Aspects of the Sustainability of Clothing Production," *Sustainability*, vol. 16, no. 20, pp. 1-30, 2024. [CrossRef] [Google Scholar] [Publisher Link]

[4] Ahmet Çay, "Energy Consumption and Energy Saving Potential in Clothing Industry," *Energy*, vol. 159, pp. 74-85, 2018. [CrossRef] [Google Scholar] [Publisher Link]

[5] S. Palamutcu, "Electric Energy Consumption in the Cotton Textile Processing Stages," *Energy*, vol. 35, no. 7, pp. 2945-2952, 2010. [CrossRef] [Google Scholar] [Publisher Link]

[6] Abdullah Al Mamun et al., "Energy Consumption Modeling in Industrial Sewing Operations: A Case Study on Carbon Footprint Measurement in the Apparel Industry," *Manufacturing Letters*, vol. 41, pp. 1635-1644, 2024. [CrossRef] [Google Scholar] [Publisher Link]

[7] Betül Özer, and Behçet Güven, "Energy Efficiency Analyses in a Turkish Fabric Dyeing Factory," *Energy Sources, Part A: Recovery, Utilization and Environmental Effects*, vol. 43, no. 7, pp. 852-874, 2021. [CrossRef] [Google Scholar] [Publisher Link]

[8] S. Sakti, B.M. Sopha, and E.S.T. Saputra, "Energy Efficiency Analysis in a Textile Company Using DMAIC Approach," *IOP Conference Series: Materials Science and Engineering*, vol. 1096, no. 1, pp. 1-12, 2021. [CrossRef] [Google Scholar] [Publisher Link]

[9] R. Korycki, and H. Szafrańska, "Optimisation of Pad Thicknesses in Ironing Machines during Coupled Heat and Mass Transport," *Fibres and Textiles in Eastern Europe*, vol. 24, no. 1, pp. 128-135, 2016. [CrossRef] [Google Scholar] [Publisher Link]

[10] Zhibin Xie, and Baoshou Sun, "Research of Ironing Product by Saturated Steam Thermal Energy," *Proceedings of the 2010 International Conference on Measuring Technology and Mechatronics Automation*, Changsha, China, pp. 1087-1090, 2010. [CrossRef] [Google Scholar] [Publisher Link]

[11] Changsang Yun et al., "Sustainable Care of Textile Products and Its Environmental Impact: Tumble-Drying and Ironing Processes," *Fibers and Polymers*, vol. 18, no. 3, pp. 590-596, 2017. [CrossRef] [Google Scholar] [Publisher Link]